Journal of Electroceramics
https://doi.org/10.1007/s10832-019-00192-5

Structure and microwave dielectric properties of double vanadate $Ca_9A(VO_4)_7$ (A= La, Pr, Nd and Sm) ceramics for LTCC applications

R. Naveenraj[1] · A. N. Unnimaya[1] · E. K. Suresh[1] · R. Ratheesh[2]

Received: 8 February 2019 / Accepted: 14 November 2019

Abstract
$Ca_9A(VO_4)_7$ (A = La, Pr, Nd and Sm) ceramics have been prepared by conventional solid state ceramic route. The phase purity of the samples was confirmed by powder X-ray diffraction technique. Raman spectroscopic studies confirm the existence of $(VO_4)^{3-}$ vibrational groups in $Ca_9A(VO_4)_7$ ceramics. $Ca_9A(VO_4)_7$ (A = La, Pr, Nd and Sm) ceramics exhibit microwave dielectric properties of $\varepsilon_r = 9.8$ to 10.4, Qxf = 4500 to 14,900 GHz and low temperature coefficient of resonant frequency $\tau_f = -3.8$ to −10.2 ppm/°C. $Ca_9A(VO_4)_7$ ceramics with A = La, Nd and Sm show good chemical compatibility with Ag electrode and can be used as candidate materials for LTCC applications.

Keywords Ceramics · Sintering · X-ray diffraction · Raman spectroscopy · Dielectric properties

1 Introduction

With the rapid advancement of miniaturized devices in the wireless communication industry, the search for novel dielectric materials with stable dielectric properties have become important for microwave/mm wave communication devices. In this context, multilayer co-fired ceramics have been widely used for several devices such as band pass filters, capacitors, oscillators, dielectric waveguides etc., to meet the demand for the miniaturization of microwave communication systems. Low temperature co-fired ceramics (LTCC) technology has become a significant approach for miniaturization because of its ease of fabrication and integration of electronic components with desirable properties. The important characteristics required for LTCC ceramics for practical applications include low dielectric constant, high quality factor, near zero temperature coefficient of resonant frequency, low sintering temperature well below the melting point of silver metal electrode, chemical compatibility with metal electrode etc. [1, 2]. Among these, chemical compatibility with metal electrode is one of the decisive parameters for LTCC applications. Commercial LTCC materials usually use highly conductive silver as metal electrode. Therefore, it is important to develop microwave dielectric ceramics that have sintering temperature below the melting point of silver (961 °C) while maintaining good dielectric properties for practical applications [3]. The conventional materials that have already used in wireless communication systems with good microwave dielectric properties are evicted from LTCC application point of view because of their high sintering temperatures (≥1300 °C) [4, 5]. Additives such as glass and low melting oxides effectively reduce the sintering temperature of dielectric ceramic, but such additives often adversely affect the microwave dielectric properties especially the intrinsic quality factor of the ceramics [6, 7]. This accelerates the need for new glass-free LTCC materials with improved properties together with low sintering temperatures for multilayer integrated circuit applications.

Recently, several dielectric ceramics based on TeO_2, Li_2O, Bi_2O_3, MoO_3 and V_2O_5 have been developed as promising candidate materials for LTCC applications because of their low sintering temperatures [8–23]. In spite of the low sintering temperature and reasonably good microwave dielectric properties, tellurium based dielectrics have serious downside of toxicity and poor compatibility with silver electrode [10]. These drawbacks limit their further applications in the field of LTCC, which leads to the search for new ceramic systems

✉ R. Ratheesh
ratheesh@cmet.gov.in; http://www.cmet.gov.in

[1] Microwave Materials Group, Centre for Materials for Electronics Technology (C-MET), Ministry of Electronics and Information Technology, Government of India, Athani P.O, Thrissur, Kerala 680581, India

[2] Centre for Materials for Electronics Technology (C-MET), Ministry of Electronics and Information Technology, Government of India, Hyderabad, Telangana 500051, India

Published online: 05 December 2019

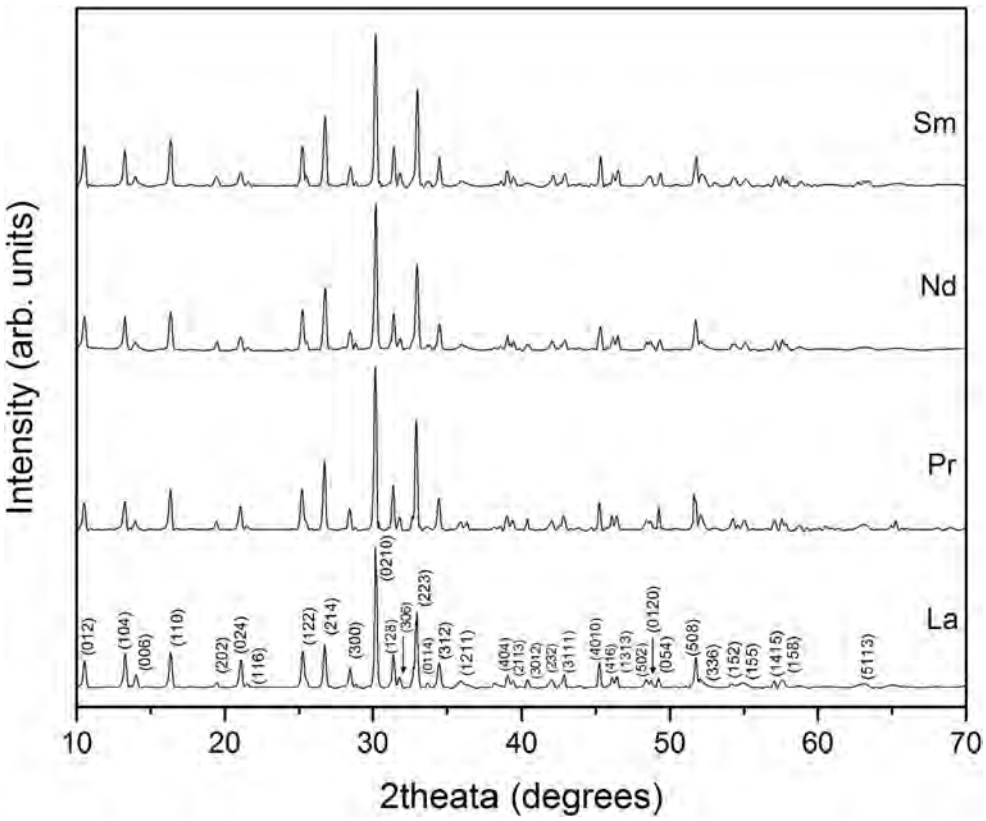

Fig. 1 (a-d) XRD patterns of $Ca_9A(VO_4)_7$(A = La, Pr, Nd and Sm) ceramics.

with better microwave dielectric properties and chemical compatibility. Very recently, many Ultra low temperature co-fired (ULTCC) ceramics are reported in literature which are prepared through conventional solid state ceramic as well as cold sintering processes with reasonably good microwave dielectric properties [11, 15, 17, 18]. Among these, vanadium based dielectric ceramics gained considerable attention owing to their excellent chemical compatibility with silver electrode [20–23].

Double Vanadates $Ca_9A(VO_4)_7$, where A can be a trivalent rare earth cation or Bi^{3+} ion was first reported by Belik et al. [24–26]. According to their reports, $Ca_9A(VO_4)_7$ compounds are isostructural with that of $Ca_3(VO_4)_2$ (R3c space group; a = 10.809 Å and c = 38.028 Å), which adopts Whitlockite type structure without any inversion centre. $Ca_9A(VO_4)_7$ compounds crystallize in the trigonal system with R3c space group with six molecules per unit cell (Z = 6). Later, the detailed crystal structure of $Ca_9A(VO_4)_7$ is reported using Rietveld refinement by Evans et al. [27]. As per their reports, the crystal structure of $Ca_9A(VO_4)_7$ compounds belong to trigonal symmetry, R3c space group with Z = 6. Structural refinement by Evans et al. suggests that double vanadate compositions can accommodate rare earth atoms in the Ca site by assigning a partial occupancy of calcium and rare earth cations. Among the structurally characterized phases in Ca/A/V/O quaternary system, all the $Ca_9A(VO_4)_7$ phases show efficient second harmonic generation, indicating its potential use as nonlinear optical material [24–27]. Recently, the spectral and photoluminescent properties of $Ca_9A(VO_4)_7$ with A = La, Gd and Y are reported by many researchers [28–30]. On the other hand,

Table 1 Calculated lattice parameters of $Ca_9A(VO_4)_7$ (A = La, Pr, Nd and Sm) ceramics

A	Ionic radius (Å)	Calculated lattice parameters (Å)		Reported lattice parameters (Å)		Molar Volume Å^3	c/a ratio
		a = b	c	a = b	c		
La	1.032	10.842	38.140	10.898	38.147	3882.66	3.518
Pr	0.990	10.839	38.129	10.881	38.135	3879.39	3.517
Nd	0.983	10.837	38.064	10.872	38.121	3871.36	3.514
Sm	0.958	10.832	37.994	10.865	38.098	3860.67	3.508

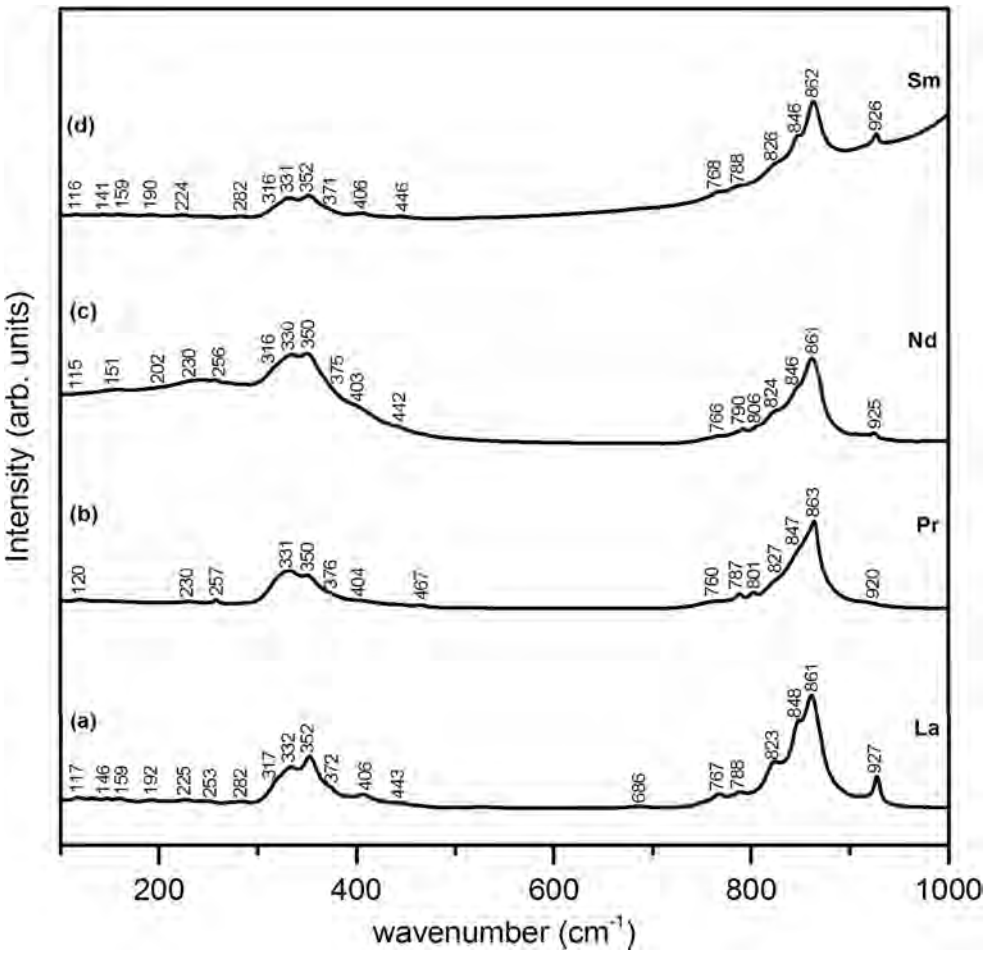

Fig. 2 (a-d) Raman spectra of $Ca_9A(VO_4)_7$ (A = La, Pr, Nd and Sm) ceramics.

there are no reports available on the microwave dielectric properties of $Ca_9A(VO_4)_7$ compounds to the best of our knowledge.

Depending on the ionic radii of A^{3+} ions, $Ca_9A(VO_4)_7$ (A = rare earth element) compounds are divided in to two groups, compounds containing A = La- Eu belong to the first group and compounds with A = Tb-Y belong to the second group [25, 26]. Owing to the interesting structural features of these materials system, we have carried out a systematic study on the structure and microwave dielectric properties of $Ca_9A(VO_4)_7$ compounds belongs to the first group, where A = La, Pr, Nd and Sm with an objective to develop new vanadate microwave ceramic materials for LTCC applications.

2 Experimental procedure

$Ca_9A(VO_4)_7$ ceramics (A = La, Pr, Nd and Sm) were prepared by conventional solid state ceramic route using high purity oxides and carbonates such as $CaCO_3$ (Sigma Aldrich, 99%), La_2O_3 (Sigma Aldrich, 99.9%), Pr_6O_{11} (Aldrich, 99.9%), Nd_2O_3 (Aldrich, 99.9%), Sm_2O_3 (Sigma Aldrich, 99%) and V_2O_5 (Sigma Aldrich, 99%) as starting materials. Stoichiometric amounts of the raw materials were weighed and wet mixed in distilled water for an hour in an agate mortar. The resultant slurry was dried, then ground well, and calcined at 600 °C for 1 h. The calcined powders were ground again and then mixed with 5 wt% polyvinyl alcohol (PVA) as binder and dried well. The granulated powders were pressed uniaxially in an 11 mm diameter tungsten carbide (WC) die by applying a pressure of 250 MPa in a hydraulic hand press. These cylindrical green compacts were sintered in a programmable furnace at various temperatures. The green compacts were fired at a rate of 5 °C/min up to the sintering temperature and an intermediate soaking was given at 600 °C for 30 min to expel the binder (PVA).

Phase purity of the $Ca_9A(VO_4)_7$ samples were studied by powder X-ray diffraction (XRD) measurement using CuK_α radiation (Bruker 5005, Germany). The Raman spectra of the ceramic compositions under study were recorded using a Thermo Scientific DXR with Nd: YVO_4

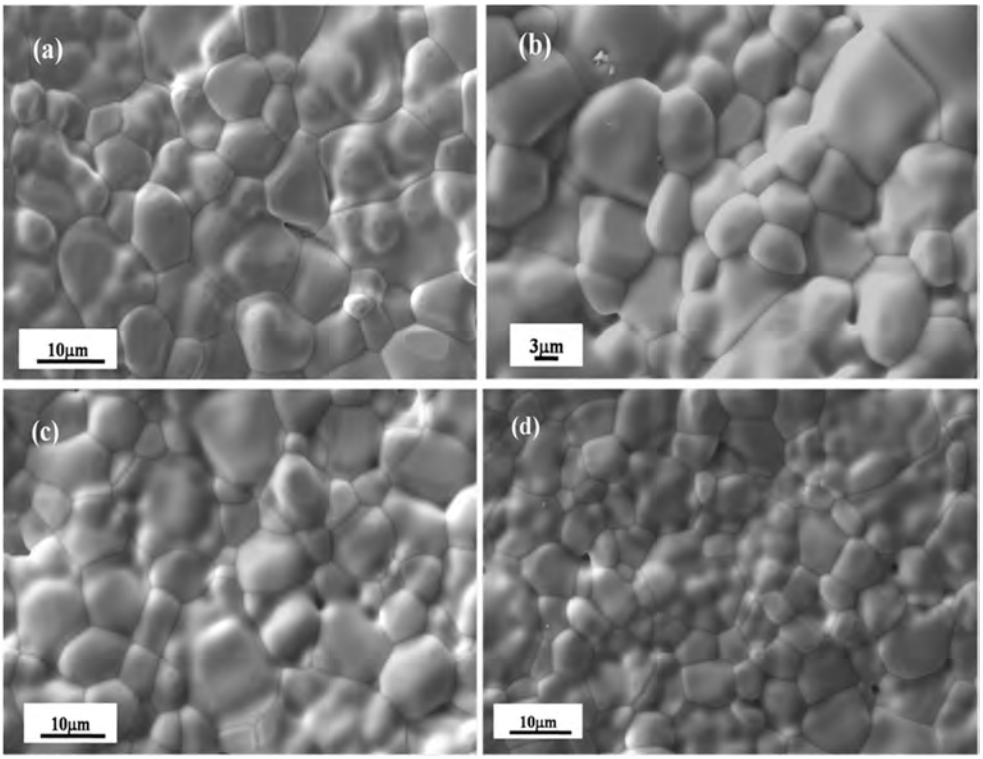

Fig. 3 SEM images of sintered $Ca_9A(VO_4)_7$ ceramics with (a) La at 940 °C (b) Pr at 1000 °C (c) Nd at 940 °C and (d) Sm at 940 °C for 1 h

DPSS laser of 532 nm. The surface morphology of the sintered samples was studied using scanning electron microscopy (Carl Zeiss, Germany). The microwave dielectric properties were measured using a vector network analyzer (Agilent make PNA E8362B, Bayan Lepas, Malaysia). The dielectric constant and the unloaded quality factor of the samples were measured by Hakki and Coleman post resonator and resonant cavity methods respectively [31, 32]. The temperature coefficient of resonant frequency (τ_f) was also measured by noting the variation of $TE_{01\delta}$ mode frequency with temperature in the range of 30–100 °C.

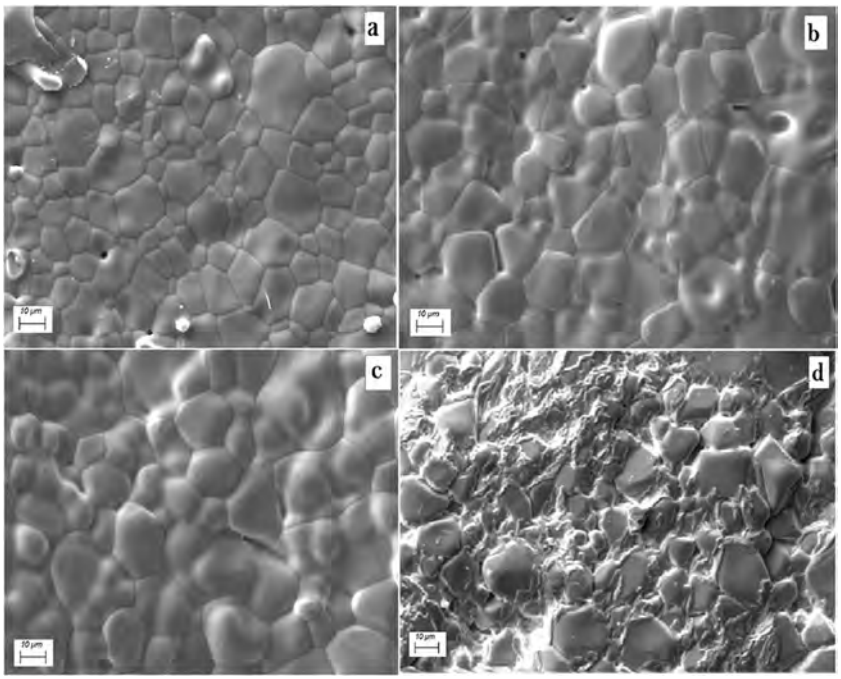

Fig. 4 SEM images of $Ca_9La(VO_4)_7$ ceramic sintered at (a) 920 °C (b) 930 °C (c) 940° and (d) 950 °C for 1 h

Table 2 Sintering temperature, density and microwave dielectric properties of $Ca_9A(VO_4)_7$ (A = La, Pr, Nd and Sm) ceramics

A element	Sintering Temp. (°C)/1 h	Density (g/cm^3)	% of Density	(ε_r) at GHz	ε_{theo}	$Q_u$xf (GHz)	τ_f (ppm/°C)
La	940	2.92	90	10.4	8.71	4500	−10.2
Pr	1000	2.80	87	10.1	8.55	14,900	−6.1
Nd	940	2.87	88	10	8.54	6800	−4.4
Sm	940	2.88	89	9.8	8.53	9100	−3.8

3 Results and discussions

Figure 1(a-d) shows the powder X-ray diffraction patterns of $Ca_9A(VO_4)_7$ (A = La, Pr, Nd and Sm) ceramics sintered at different temperatures. Among the double vanadate ceramics, the crystal structure of $Ca_9A(VO_4)_7$ with A = La, Pr, Nd and Sm is reported by Belik et al. [24–26]. The available XRD pattern of $Ca_9La(VO_4)_7$ (ICDD Card No. 46–0410) is exactly matches with that of $Ca_9La(VO_4)_7$ prepared in the present study and hence indexed based on the same. According to the available structural studies of double vanadate samples, $Ca_9A(VO_4)_7$ with A = Pr, Nd and Sm are found to be isostructural with that of $Ca_9La(VO_4)_7$. In the present study also, XRD patterns of $Ca_9A(VO_4)_7$ with A = Pr, Nd and Sm are exactly match with the available ICDD pattern of $Ca_9La(VO_4)_7$. No detectable amount of secondary phases was found in the XRD patterns, which clearly indicates the phase purity of the compositions under study. The calculated lattice parameters of $Ca_9La(VO_4)_7$ are a = b = 10.842 Å and c = 38.140 Å, which are in good agreement with the available ICDD data.

Table 1 shows the variation in the lattice parameters of $Ca_9A(VO_4)_7$ ceramics with different A^{3+} ions. It can be seen that there is a systematic variation in the lattice parameters with decrease in the ionic radii of A^{3+} ions. The hkl values of $Ca_9A(VO_4)_7$ ceramics in the XRD patterns are also shifted to higher 2θ values while substituting A^{3+} ions from La to Sm due to the contraction of the unit cell volume as a result of decrease in ionic radii [33–36]. The calculated lattice parameter values and c/a ratio of $Ca_9A(VO_4)_7$ (A = La, Pr, Nd and Sm) ceramics prepared in the present study show good consistency with those previously reported by Belik et al. [24, 25].

In order to understand the crystal structure of $Ca_9A(VO_4)_7$ compositions in the molecular level, Laser Raman spectra of these compositions have been recorded. Figure 2(a-d) shows the Laser Raman spectra of $Ca_9A(VO_4)_7$ (A = La, Pr, Nd and Sm) ceramics.

The crystal structural studies of $Ca_9A(VO_4)_7$ ceramics by Belik et al. reveal that double vanadate ceramics with mixed ionic-covalent bonding belong to mineral whitlockite structure and are isostructural to $Ca_3(VO_4)_2$. The structure of $Ca_3(VO_4)_2$ contains isolated $(VO_4)^{3-}$ tetrahedrons where the Ca^{2+} ions occupy the 5 non-equivalent crystallographic positions M(1)-M(5) and the coordination numbers are 7, 8, 8 and 8 for the M(1)-M(3), M(5) positions and the M(4) position is half filled. According to their reports, the formation of $Ca_9A(VO_4)_7$ compounds is accompanied with the heterovalant substitution of Ca^{2+} ions by A^{3+} ions according to the scheme $3Ca^{2+}$ =

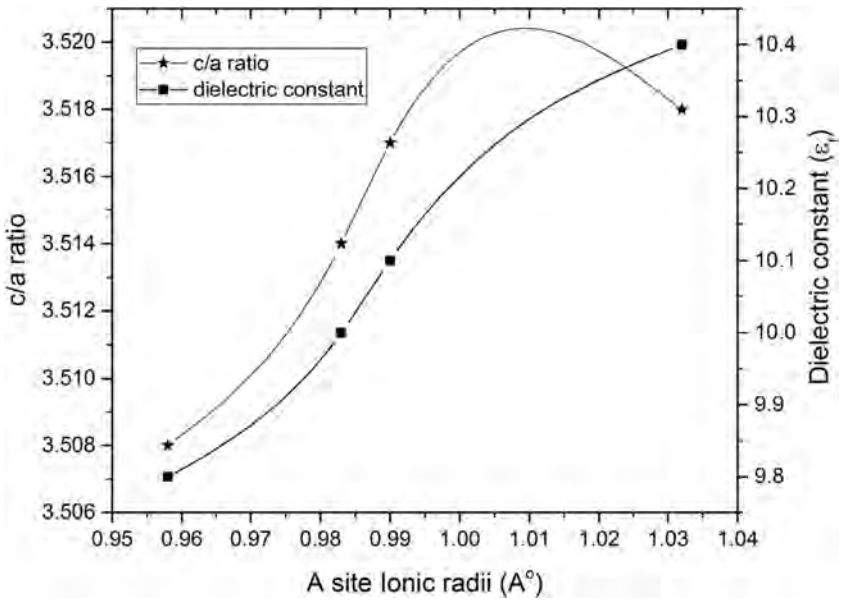

Fig. 5 Variation of c/a ratio and dielectric constant of $Ca_9A(VO_4)_7$ (A = La, Pr, Nd and Sm) ceramics with ionic radii of A ions

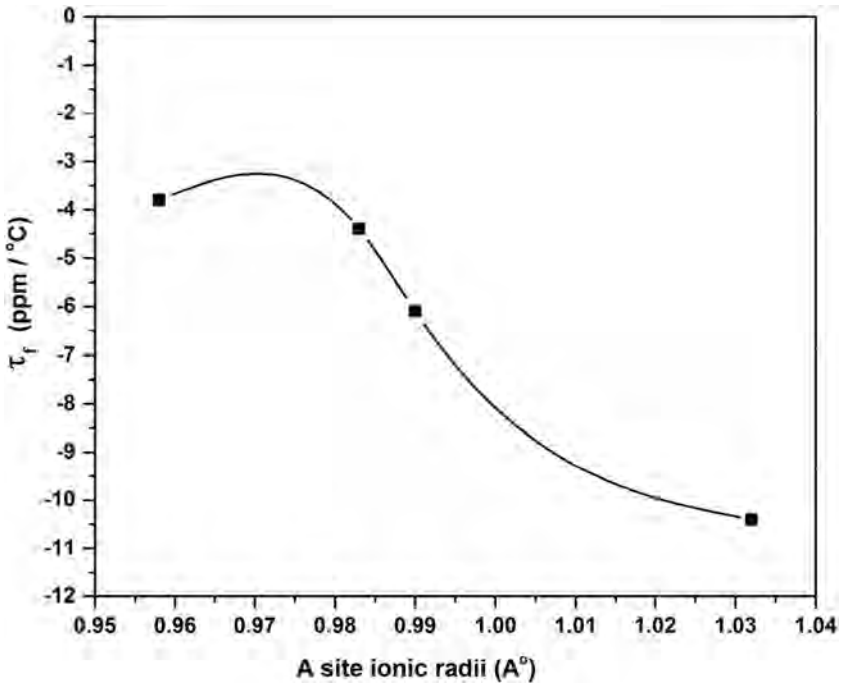

Fig. 6 Variation of temperature coefficient of resonant frequency of $Ca_9A(VO_4)_7$ (A = La, Pr, Nd and Sm) ceramics with ionic radii of A ions

$2A^{3+}$ + o where 'o' is a vacancy. Hence, the partially filled Ca(4) site in $Ca_3(VO_4)_2$ is completely vacant in $Ca_9A(VO_4)_7$ compounds, where calcium and rare-earth metal cations occupy statistically three sites in the structure and the site occupancies depend on the radius of the A^{3+} cations [24].

The Raman spectra of double vanadates in the present study show close resemblance with that of $Ca_3(VO_4)_2$ which is extensively studied by A. Grzechnik [37]. Structural studies of double vanadates by Evans et al. confirm the existence of VO_4 tetrahedra with an average V-O bond length of 1.71 Å and an average A-O distance of 2.52 Å in $Ca_9A(VO_4)_7$ compounds [21]. Hence, the vibrational modes observed in the $Ca_9A(VO_4)_7$ compounds can be attributed due to the VO_4 tetrahedra of the double vanadates. Raman spectrum of $Ca_9La(VO_4)_7$ have four symmetric stretching vibrations at 927, 861, 848 and 823 cm^{-1} and three asymmetric stretching vibrations at 787, 767 and 750 cm^{-1} whereas an additional

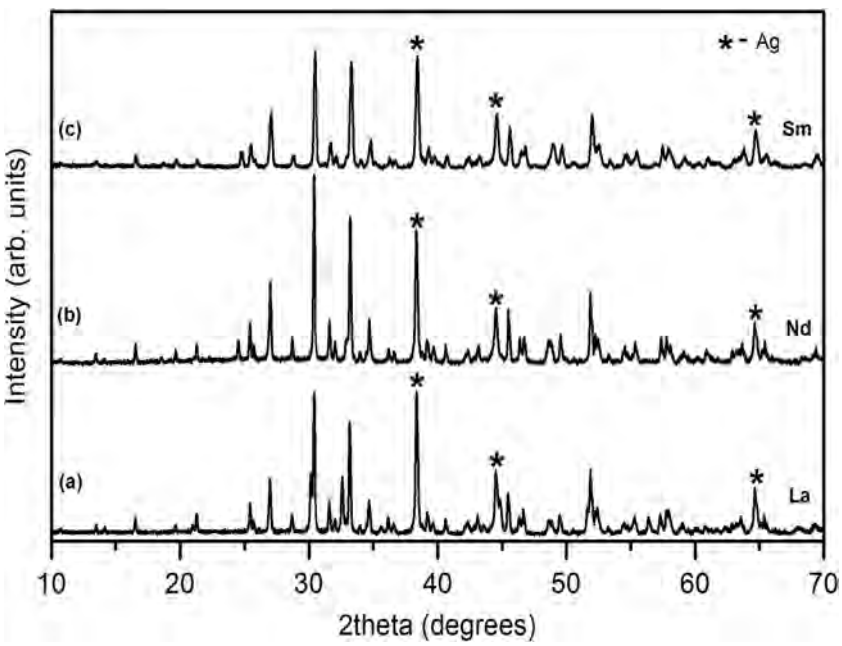

Fig. 7 XRD patterns of $Ca_9A(VO_4)_7$ (A = La, Nd and Sm) + 20 wt% Ag ceramics sintered at optimum sintering temperatures

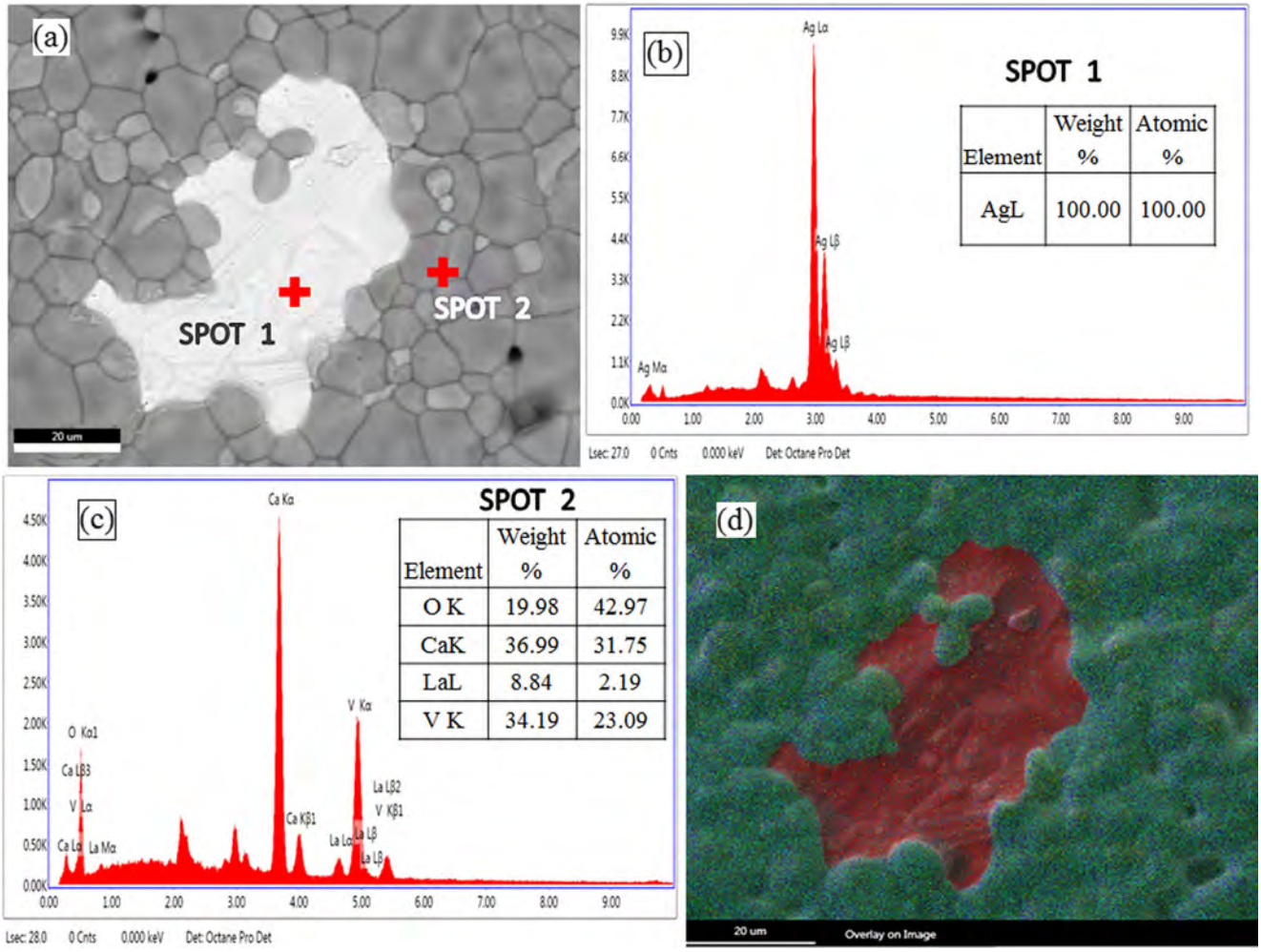

Fig. 8 (a) SEM image of $Ca_9La(VO_4)_7$ ceramic co-fired with 20 wt% Ag (b) EDS spectrum of spot 1 (c) EDS spectrum of spot 2 and (d) X-ray dot mapping of $Ca_9La(VO_4)_7$ ceramic co-fired with 20 wt% Ag

symmetric stretching mode is observed at 801 cm^{-1} in the Raman spectrum of $Ca_9Pr(VO_4)_7$. The Raman spectrum of $Ca_3(VO_4)_2$ have similar symmetric and asymmetric stretching vibrations together with an additional mode at 911 cm^{-1} whereas asymmetric stretching vibration at 750 cm^{-1} is absent in calcium orthovanadate compared to the double vanadate sample [37]. Recently, the Raman spectrum of $Ca_9Nd(VO_4)_7$ is reported for the first time by Demesh et al. [38]. They confirm the existence of distorted VO_4 tetrahedra in $Ca_9Nd(VO_4)_7$ ceramic. The Raman spectrum of $Ca_9Nd(VO_4)_7$ in the present study matches with the already reported result of Demesh et al. Further, the Raman spectrum of $Ca_9Sm(VO_4)_7$ also have stretching and bending vibrations of $(VO_4)^{3-}$ groups similar to that of $Ca_9La(VO_4)_7$ which clearly indicates the isostructural nature of double vanadate ceramics with A = La, Pr, Nd and Sm.

Figure 3 (a-d) shows the SEM micrographs of $Ca_9A(VO_4)_7$ (A = La, Pr, Nd and Sm) ceramics at optimum sintering temperatures. All the $Ca_9A(VO_4)_7$ ceramics exhibit dense microstructure with closely packed polygonal grains having an average grain size of 5-10 μm. No indications of secondary phases are observed in the microstructure of the double vanadate ceramics.

The SEM pictures of $Ca_9La(VO_4)_7$ ceramic sintered at various temperatures are given in Fig. 4(a-d). It is clearly visible from the micrographs that melted appearance is seen in ceramics which are sintered beyond optimum temperature ie. 940 °C (Fig.4(c-d)) whereas porosity is seen in sample sintered below the optimum temperature. Hence in the present study, detailed microwave dielectric property evaluation is carried out on optimum sintered samples.

Microwave dielectric properties of the sintered $Ca_9A(VO_4)_7$ (A = La, Pr, Nd and Sm) ceramics were measured using a vector network analyzer. The optimum sintering temperature, density, dielectric constant, quality factor and temperature coefficient of resonant frequency of the ceramics under study are compiled in Table 2. According to Belik et al.,

$Ca_9A(VO_4)_7$ double vanadates formation occurs at relatively higher temperature range of 900–1000 °C [24–26]. Among the compositions studied, $Ca_9Pr(VO_4)_7$ ceramic is sintered at an optimum temperature of 1000 °C for 1 h whereas all other compounds sinter below 960 °C. The dielectric constant values of the double vanadate ceramics are also theoretically calculated using following Clausius-Mossotti relation

$$\varepsilon_r = \frac{3V_m + 8\pi\alpha_D}{3V_m - 4\pi\alpha_D} \quad (1)$$

Where α_D is dielectric polarizability of the compound and V_m is the molar volume calculated from lattice parameters [39–42]. The calculated dielectric constant values of $Ca_9A(VO_4)_7$ ceramics are shown in Table 2.

From Table 2 it is clear that the experimental dielectric constant is greater than the calculated dielectric constant values for the double vanadate samples. Clausius- Mossotti relation is derived based on Cubic structure and the deviation of calculated dielectric constant from the experimental result may be due to the lower symmetry of the present samples under study.

Figure 5 shows the variation of c/a ratio and dielectric constant of $Ca_9A(VO_4)_7$ ceramics with ionic radius of A^{3+}cation. Both c/a ratio and dielectric constant of the double vanadate ceramics exhibited similar trend. The dielectric constant and lattice volume show an increasing trend as a result of increase in the ionic radii of the rare earth ions. The higher ionic polarizability (α_D) of A^{3+} ions from Sm^{3+} to La^{3+} and increase in molar volume as a function of ionic radii are the reasons for the monotonous of increase of dielectric constant [41–43]. It is clear from Table 2 that among the $Ca_9A(VO_4)_7$ ceramics, a maximum Qxf value of 14,900 GHz was observed for $Ca_9Pr(VO_4)_7$ ceramic sintered at 1000 °C for 1 h.

Figure 6 shows the variation of τ_f values of $Ca_9A(VO_4)_7$ ceramics with various A^{3+} elements. The τ_f values of $Ca_9A(VO_4)_7$ ceramics are varied from -10 ppm/°C to near zero τ_f value as a result of decrease in values of the ionic radii of the A^{3+} cations. The τ_f values observed in the present work is very low compared to other LTCC vanadate compositions reported in the literature and hence can be used for outdoor wireless applications [16, 20, 23].

In order to use $Ca_9A(VO_4)_7$ (A = La, Nd and Sm) ceramics for LTCC applications, chemical compatibility with metal electrode is very important. In order to evaluate the chemical compatibility, $Ca_9A(VO_4)_7$ with A = La, Nd and Sm were co-fired with 20 wt% Ag powder at 940 °C for 1 h. The X-ray diffraction patterns of the co-fired double vanadate samples given in Fig. 7 show silver peaks separately and are marked with '*', which rules out the possibility of secondary phase formation in the co-fired samples.

Out of the double vanadate samples, the co-fired $Ca_9La(VO_4)_7$ sample was subjected to EDS (energy-dispersive spectroscopy) analysis and the result is given in Fig. 8. Spot 1 shows the segregation of melted Ag particles whereas Spot 2 represents well-formed grains of the $Ca_9La(VO_4)_7$ ceramic respectively. It is clear from the EDS spectra that there is no inter-diffusion of Ag into the ceramic phase. X-ray dot mapping of the co-fired sample was also carried out to further quantify the compatibility. Mapping studies confirm the segregation of Ag particles and the non-reactivity of Ag in the double vanadate ceramic.

4 Conclusion

$Ca_9A(VO_4)_7$ (A = La, Pr, Nd and Sm) ceramics have been prepared through conventional solid state ceramic route. The phase purity of the samples was confirmed by powder X-ray diffraction techniques. Raman spectroscopic studies confirm the existence of $(VO_4)^{3-}$ vibrational groups in $Ca_9A(VO_4)_7$ ceramics. Among the compositions studied, $Ca_9A(VO_4)_7$ (A = La, Nd and Sm) ceramics were well sintered below 960 °C. All the $Ca_9A(VO_4)_7$ ceramics under study exhibit relatively low dielectric constant and negative temperature coefficient of resonant frequency (τ_f). Among the studied samples, $Ca_9Pr(VO_4)_7$ ceramic exhibits highest quality factor Qxf = 14,900 GHz compared to other double vanadate samples. The EDS analyses reveal good chemical compatibility between calcium double vanadate ceramic and Ag electrode. The present study shows that, $Ca_9A(VO_4)_7$ with A = La, Nd and Sm ceramics can be used as suitable candidate materials for LTCC applications.

Acknowledgements The authors are thankful to Dr. N. Raghu, Director, C-MET, Thrissur for extending the facilities to carry out the work. The authors are also thankful to the Board of Research in Nuclear Sciences, Mumbai for financial support under grant number 34/15/01/2014-BRNS/0906. One of the authors, E.K.Suresh is grateful to the Council of Scientific and Industrial Research (CSIR), India for the award of Senior Research Fellowship.

References

1. M.T. Sebastian, H. Jantunen, Int. Mater. Rev. **53**(2), 57–90 (2008)
2. K. Wakino, Ceram. Trans. **100**, 499–506 (1999)
3. M. Valant, D. Suvorov, J. Am, Ceram. Soc. **83**(11), 2721–2729 (2000)
4. M.T. Sebastian, K.P. Surendran, J. Eur, Ceram. Soc. **26**(10), 1791–1799 (2006)
5. J. Takada, S.F. Wang, S. Yoshikawa, S.J. Jang, R.E. Newnham, J. Am, Ceram. Soc. **77**(9), 2485–2488 (1994)
6. C.L. Huang, K.H. Chiang, S.C. Chuang, Mat. Res. Bull. **39**(4–5), 629–636 (2004)
7. K.P. Surendran, P. Mohanan, M.T. Sebastian, J. Solid State Chem. **177**(11), 4031–4036 (2004)
8. M. Udovic, M. Valant, D. Suvorov, J. Am, Ceram. Soc. **87**(4), 591–597 (2004)
9. D.K. Kwon, M.T. Lanagan, T.R. Shrout, J. Am, Ceram. Soc. **88**(12), 3419–3422 (2005)

10. G. Subodh, M.T. Sebastian, J. Am, Ceram. Soc. **90**(7), 2266–2268 (2007)
11. S.S. Faouri, A. Mostaed, J.S. Dean, D. Wang, D.C. Sinclair, S. Zhang, W.G. Whittow, Y. Vardaxoglou, I.M. Reaney, Acta Mater. **166**, 202–207 (2019)
12. N.K. James, R. Ratheesh, J. Am, Ceram. Soc. **93**(4), 931–933 (2010)
13. D. Zhou, C.A. Randall, L.X. Pang, H. Wang, J. Guo, G.Q. Zhang, X.G. Wu, L. Shui, X. Yao, J. Am, Ceram. Soc. **94**(2), 348–350 (2011)
14. D. Zhou, D. Guo, W.B. Li, L.X. Pang, X. Yao, D.W. Wang, I.M. Reaney, J. Mater, Chem. C. **4**(23), 5357–5362 (2016)
15. D. Wang, S. Zhang, D. Zhou, K. Song, A. Feteira, Y. Vardaxoglou, W.G. Whittow, D. Cadman, I.M. Reaney, Materials (Basel) **12**(9), 1370–1380 (2019)
16. D. Zhou, L.X. Pang, D.W. Wang, I.M. Reaney, J. Mater, Chem. C **6**(35), 9290–9313 (2018)
17. D.W. Wang, D. Zhou, S. Zhang, Y. Vardaxoglou, W.G. Whittow, D. Cadman, I.M. Reaney, ACS Sustainable Chem. Eng. **6**(2), 2438–2444 (2018)
18. D. Zhou, L.X. Pang, D.W. Wang, I.M. Reaney, J. Eur, Ceram. Soc. **39**(7), 2374–2378 (2019)
19. D. Zhou, H. Wang, X. Yao, L.X. Pang, J. Am, Ceram. Soc. **91**(10), 3419–3422 (2008)
20. E.K. Suresh, A.N. Unnimaya, R Ratheesh. Ceram. Int. **39**(4), 3635–3639 (2013)
21. E.K. Suresh, A.N. Unnimaya, R. Ratheesh, J. Am, Ceram. Soc. **97**(5), 1530–1533 (2014)
22. A.N. Unnimaya, E.K. Suresh, R. Ratheesh, Eur. J. Inorg. Chem. **2015**(2), 305–310 (2015)
23. M.T. Sebastian, H. Wang, H. Jantunen, Curr. Opin. Solid State Mater. Sci. **20**(3), 151–170 (2016)
24. A.A. Belik, V.A. Morozov, R.N. Kotov, S.S. Khasanov, B.I. Lazoryak, Crystallogr. Rep. **42**(5), 751–757 (1997)
25. A. A. Belik, V. A. Morozov, N. Kotov, S. S. Khasanov, B. I. Lazoryak, Crystallogr. Rep. **45**(3), 389–394 (2000) [Translated from Kristallografiya, **45**(3), 432–437 (2000)]
26. A. A. Belik, V. A. Morozov, S. V. Grechkin, S. S. Khasanov, B. I. Lazoryak, Crystallogr. Rep **45**(5), 728–733 (2000) [Translated from Kristallografiya, **45**(5),798–803 (2000)]
27. J.S.O. Evans, J. Huang, A.W. Sleight, J. Solid State Chem. **157**(2), 255–260 (2001)
28. R. Singh, S.J. Dhoble, J. Lumin, Luminescence **28**(4), 607–613 (2013)
29. S. Cao, Y. Ma, C. Quan, W. Zhu, K. Yang, W. Yin, G. Zheng, M. Wu, Z. Sun, J. Alloy, Compds. **487**(1–2), 346–350 (2009)
30. X. Wu, Y. Huang, L. Shi, H.J. Seo, J. Mate, Chem. Phys. **116**(2–3), 449–452 (2009)
31. B.W. Hakki, P.D. Coleman, IRE Trans. Microw. Theory. Tech. **8**(4), 402–410 (1960)
32. J. Mazierska, M.V. Jacob, A. Harring, J. Krupka, P. Barnwell, T. Sims, J. Eur, Ceram. Soc. **23**(14), 2611–2615 (2003)
33. S. Thomas, M.T. Sebastian, J. Am, Ceram. Soc. **92**(12), 2975–2981 (2009)
34. S.C. Shirbhate, A.K. Yadav, S.A. Acharya, Appl. Phys. Lett. **108**(14), 143501–143505 (2016)
35. S.D. Ramarao, V.R.K. Murthy, Scr. Mater. **69**(3), 274–277 (2013)
36. S.D. Ramarao, S.R. Kiran, V.R.K. Murthy, Mat. Res. Bull. **56**, 71–79 (2014)
37. A. Grzechnik, Chem. Mater. **10**(4), 1034–1040 (1998)
38. M.P. Demesh, A.S. Yasukevich, N.V. Kuleshov, M.B. Kosmyna, P.V. Mateychenko, B.P. Nazarenko, A.N. Shekhovtsov, A.A. Kornienko, E.B. Dunina, V.A. Orlovich, I.A. Khodasevich, W. Paszkowicz, A. Behrooz, Opt. Mater. **60**(1), 387–393 (2016)
39. R.D. Shannon, J. Appl, Phys. **73**, 348–366 (1993)
40. S.D. Ramarao, S.R. Kiran, V.R.K. Murthy, J. Am, Ceram. Soc **95**(11), 1–6 (2012)
41. S.K. Singh, S.R. Kiran, V.R.K. Murthy, Mater. Chem. Phys. **141**(2–3), 822–827 (2013)
42. S.K. Singh, V.R.K. Murthy, Mater. Chem. Phys. **160**, 187–193 (2015)
43. K.P. Surendran, S. Soloman, M.R. Varma, P. Mohanan, M.T. Sebastian, J. Mater, Res **17**(10), 2561–2566 (2002)